Small-Molecule Inhibitors of the MDM2-p53 Protein−Protein Interaction Based on an Isoindolinone Scaffold

Ian R. Hardcastle,*,† Shafiq U. Ahmed,‡ Helen Atkins,‡ Gillian Farnie,‡ Bernard T. Golding,† Roger J. Griffin,† Sabrina Guyenne,† Claire Hutton,‡ Per Källblad,§ Stuart J. Kemp,† Martin S. Kitching,† David R. Newell,‡ Stefano Norbedo,† Julian S. Northen,† Rebecca J. Reid,† K. Saravanan,† Henriëtte M. G. Willems,*,§ and John Lunec*,‡

Northern Institute for Cancer Research, School of Natural Sciences−Chemistry, Bedson Building, University of Newcastle upon Tyne, Newcastle, NE1 7RU, United Kingdom, Northern Institute for Cancer Research, Paul O'Gorman Building, Medical School, Framlington Place, University of Newcastle upon Tyne, Newcastle, NE2 4HH, United Kingdom, and De Novo Pharmaceuticals, Compass House, Vision Park, Histon, Cambridge, CB4 9ZR, United Kingdom

Received February 3, 2006

From a set of weakly potent lead compounds, using in silico screening and small library synthesis, a series of 2-alkyl-3-aryl-3-alkoxyisoindolinones has been identified as inhibitors of the MDM2-p53 interaction. Two of the most potent compounds, 2-benzyl-3-(4-chlorophenyl)-3-(3-hydroxypropoxy)-2,3-dihydroisoindol-1-one (**76**; $IC_{50} = 15.9 \pm 0.8 \ \mu M$) and 3-(4-chlorophenyl)-3-(4-hydroxy-3,5-dimethoxybenzyloxy)-2-propyl-2,3-dihydroisoindol-1-one (**79**; $IC_{50} = 5.3 \pm 0.9 \ \mu M$), induced p53-dependent gene transcription, in a dose-dependent manner, in the MDM2 amplified, SJSA human sarcoma cell line.

Introduction

The p53 tumor suppressor acts as "the guardian of the genome" by reacting to cellular stress, which may be caused by hypoxia and DNA damage. This protein activates the transcription of a number of genes that govern progression through the cell cycle, the initiation of DNA repair, and programmed cell death.[1,2] The activity of p53 is tightly regulated by the MDM2 protein, which is itself transcriptionally transactivated by p53. MDM2 binds to and inactivates the p53 transactivation domain and also ubiquitylates the MDM2−p53 complex to target it for proteosomal degradation. In normal cells, the balance between active p53 and inactive MDM2-bound p53 is maintained in a negative feedback loop.[3,4]

Inactivation of p53 through mutation is common in approximately a half of all tumors. In about 7% of tumors, amplification and overexpression of the MDM2 gene results in the loss of functional p53, allowing transformation and uncontrolled tumor growth.[5] Inhibitors of the MDM2−p53 binding interaction are expected to restore normal p53 activity in MDM2-overexpressing cells and thus exert an antitumor effect.[6]

Traditionally, the disruption of protein−protein interactions has been regarded as a difficult or even impossible goal for drug development. These interactions occur over large surface areas (average $\sim 800 \ Å^2$), frequently with relatively flat topologies, typically have high binding affinities resulting from the sum of a large number of relatively weak noncovalent bonds. This suggests that each protein will be devoid of high-affinity sites for small-molecule inhibitors.[7,8] However, several examples of small-molecule antagonists of protein-receptor targets have been reported recently.[9,10] The targets include: IL-2,[11] Bcl$_{XL}$/Bax interactions,[12] p60c-src SH2 interactions with phosphorylated tyrosine residues,[13] the association of HIV-1 Tat with PCAF,[14] and bid/Bax interactions.[15]

The X-ray crystal structure of the N-terminal domain of MDM2 bound to a 15-residue peptide, corresponding to a region of the transactivation domain of p53, which had been mapped as the binding site for MDM2, revealed a relatively small binding pocket on MDM2.[16] The protein interacts with three amino acid residues within a hexapeptide region (T[18] F S D L W[23]) of p53 arrayed in an amphipathic α-helix. The tractability of this interaction as a target for small molecule inhibitors was suggested by peptide mapping experiments, which defined a hexapeptide region of p53 as the consensus sequence for MDM2 binding.[16] Phage-display peptide libraries were used to identify the 8-mer IP3 peptide (Ac-Phe[19]-Met-Asp-Tyr-Trp-Glu-Gly-Leu[26]-NH$_2$) that inhibits p53 binding to MDM2 ($IC_{50} = 9 \ \mu M$).[17] This sequence was used as a lead for the rational design of the potent AP peptide (Ac-Phe[19]-Met-Aib-Pmp-6-Cl-Trp-Glu-Ac$_3$c-Leu[26]-NH$_2$; $IC_{50} = 5$ nM) in which replacements with unnatural amino acids have been used to stabilize the α-helical structure and to introduce a salt-bridge interaction between the Pmp residue and Lys[94] outside the p53 binding domain of MDM2.[18]

A number of small-molecule inhibitors of the p53−MDM2 interaction have been reported, for example, chalcone derivatives, such as **1**, which are weak inhibitors ($IC_{50} = 49 \ \mu M$).[19] Computational methods have been used to identify potential inhibitors from combinatorial scaffolds, for example, **2**, some of which have been shown to display inhibitory activity in cell-free and cellular assays.[20,21] The natural product chlorofusin inhibits MDM2−p53 binding with an IC_{50} of 4.6 μM.[22] More recently, highly potent small-molecule inhibitors have been reported, including the Nutlins (e.g., **3a,b**),[20,22−24] and benzodiazepinediones, such as **4**.[25,26]

The cellular effects of MDM2−p53 inhibition have been investigated using a variety of agents. Inhibition of MDM2 expression with antisense oligonucleotides in cell lines with elevated and normal levels of MDM2, for example, JAR, SJSA, and MCF7 cell lines, was observed to induce increased levels of p53.[27,28] Additionally, apoptosis was observed with the JAR cells. Antisense oligonucleotides synergistically increased the potency of the DNA damaging agent camptothecin in MDM2-overexpressing and normal cell lines.[29] Peptide inhibitors have also been used to evaluate the effects of MDM2−p53 inhibition. Wasylyk et al. observed a cytotoxic effect when the IP3 peptide

* Corresponding authors: Tel.: +44 191 222 6645 (I.R.H.); +44 191 246 4420 (J.L.); +44 1223 238012 (H.W.). Fax: +44 191 8591 (I.R.H.); +44 191 4301 (J.L.); +44 1223 238088 (H.W.). E-mail: i.r.hardcastle@ncl.ac.uk (I.R.H.); john.lunec@ncl.ac.uk (J.L.); henriette.willems@denovopharma.com (H.W.).
† School of Natural Sciences−Chemistry, University of Newcastle upon Tyne.
‡ Medical School, University of Newcastle upon Tyne.
§ De Novo Pharmaceuticals.

1

2

Nutlin-2 (**3a**)

Nutlin-3 (**3b**)

4
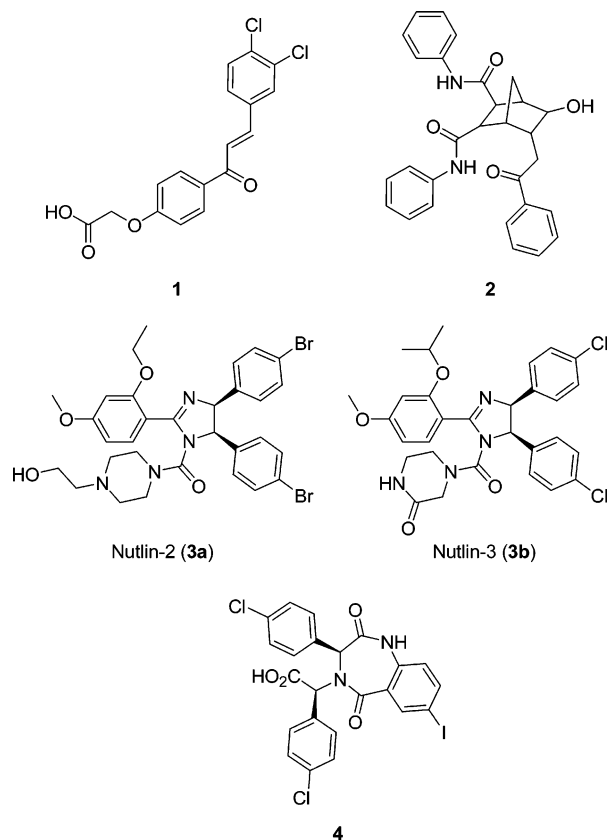
was expressed in cells.[30] The more potent AP peptide, used exogenously, has been shown to induce p53, albeit weakly, in HCT116, JAR, and SJSA-1 cell lines, which express low, intermediate, and high MDM2 levels, respectively. A large induction of the p21[Waf1/Cip1] cyclin-dependent kinase inhibitor, the gene for which is a transcriptional target of p53, was also observed in all three cell lines, but not in p53 null and p53 mutant cell lines. Induction of apoptosis was observed in the JAR and SJSA-1 cell lines.[31] Nutlin-3 was demonstrated to

induce cellular levels of p53, MDM2, and p21Waf1/Cip1 in the p53 wild-type HCT116 cell line, but not in the p53 mutant SW480. This small-molecule antagonist also showed a dose-dependent antiproliferative activity, which was dependent on the p53 status of the cell line. An in vivo antitumor effect was also demonstrated for Nutlin-3 in an MDM2 amplified SJSA-1 xenograft model at a 10 mg/kg dose.[24]

In this paper, we present a full report of the development of small-molecule inhibitors of the MDM2−p53 interaction based on an isoindolinone scaffold, which display cellular activity.[32] Preliminary screening studies, using an in vitro p53−MDM2 binding assay, identified compounds **5**, **6**, and **7** as weak inhibitors of the p53−MDM2 interaction (IC$_{50} \sim 200~\mu$M). These compounds also displayed growth inhibitory activity in the NCI 60 cell line screen, and importantly, were rated COMPARE negative with respect to any known classes of antitumor agents.[33] The versatility of the isoindolinone scaffold for the synthesis of combinatorial libraries and the availability of a high-resolution X-ray structure of the MDM2 protein target in complex with a p53-derived peptide encouraged us to pursue the optimization of this class of compounds. A program of a focused library synthesis, guided by virtual screening, has resulted in the discovery of novel isoindolinone inhibitors of the MDM2−p53 interaction with low micromolar affinity and cellular activity.
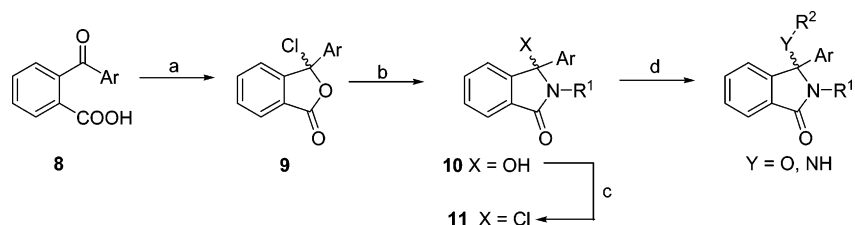

5
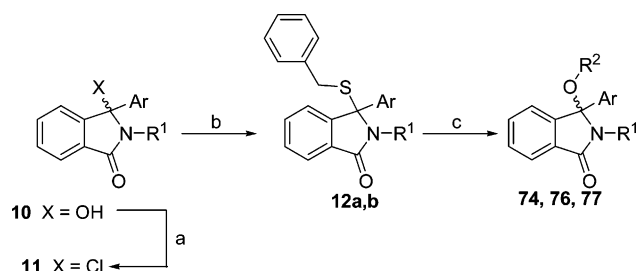
6

7
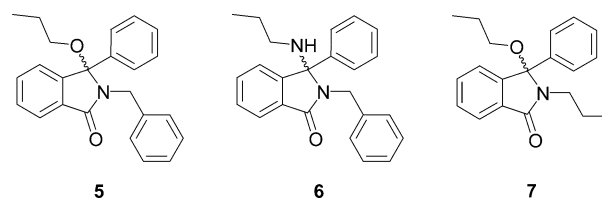
Computational Chemistry

In the absence of structural data on the isoindolinone−MDM2 interaction, docking was applied to determine a single, low-energy binding mode for the initial lead compounds **5** and **7**

Table 1. Inhibition of the MDM2−p53 Binding Interaction by Seed Compounds Used in the Second Round of Binding-Mode Determinations

Compound	Ar	R^1	X	R^2	IC$_{50}$ (μM)
13	Ph	benzyl	O	4-tert-butylphenyl	92 ± 11
14	Ph	MeO₂C-CH(CH₂-4-hydroxyphenyl)	O	propyl	90 ± 39
15	Ph	benzyl	NH	1,2-dihydroxy-2-phenylethyl	85
16	4-OSEM-phenyl	n-Pr	NH	4-tert-butylbenzoyl	27 ± 3
17	4-tert-butylphenyl	n-Pr	NH	benzoyl	66 ± 8
18	Ph	benzyl	NH	hydroxy(4-methoxyphenyl)methyl	70 ± 8

Scheme 1. Synthesis of Substituted Isoindolinones from the ψ-Acid Chloride **9**[a]

[a] Reagents and conditions: (a) $SOCl_2$, DMF, THF; (b) R^1NH_2, Et_3N, THF; (c) $SOCl_2$, DMF, THF; (d) R^2OH or R^2NH_2, K_2CO_3 or Et_3N, THF.
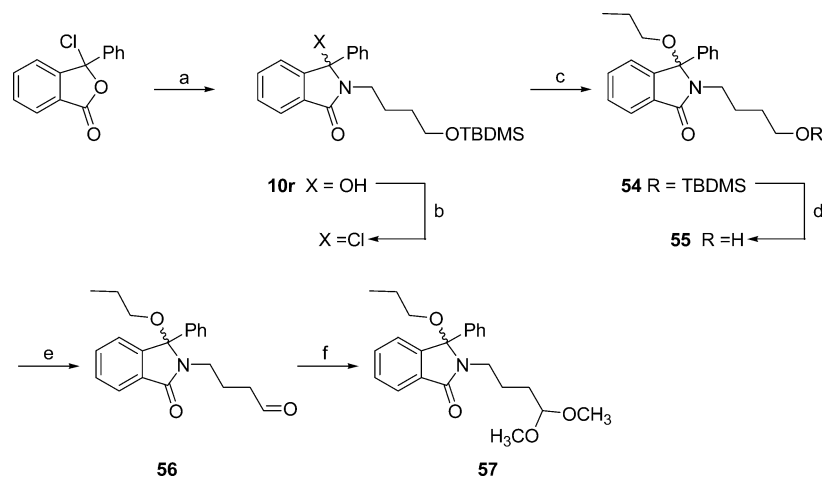
Scheme 2. Synthesis of Substituted Isoindolinones from the Thioethers **12a** and **12b**[a]

[a] Reagents and conditions: (a) $SOCl_2$, DMF, THF; (b) $PhCH_2SH$, Et_3N, THF; (c) R^2OH, NIS, CSA, THF.

Scheme 3. Synthesis of Substituted Isoindolinone **53**[a]

[a] Reagents and conditions: (a) (i) $SOCl_2$, DMF, THF; (ii) *n*-PrOH, THF; (b) TBAF, THF.

round of virtual screening of new substituents. A selection of these "virtual hits" were synthesized. Disappointingly, the compounds suggested by the virtual screening described above were no more active than a series of compounds selected for synthesis on the basis of diversity and accessibility (see Supporting Information).

The strategy for the binding mode prediction was reassessed in the light of these preliminary results. The open and lipophilic nature of the p53 binding site on MDM2 makes the determination of a single binding mode for the isoindolinone scaffold difficult. The possibility that there are multiple binding modes for the scaffold, depending on the substituents present, has to be considered. The use of multiple binding modes in this setting has been shown to increase significantly the probability of predicting correctly the experimental binding mode.[35] This approach was deemed more likely to succeed with the selection of a larger, more diverse set of "seed" compounds in the binding mode determination.

An ensemble of six "seed" compounds were used, with an IC_{50} range from 27 to 92 μM (**8**−**13**; Table 1), as the basis for a second round of virtual screening. Each of these compounds was docked into the MDM2 crystal structure 1YCR,[16] using the programs easyDock[34] and GOLD,[36] again resulting in a large number of solutions. A total of 24 high-scoring, unique binding modes were chosen providing starting points for the second round of virtual screening, that is, one binding mode per compound, stereoisomer, and docking program combination.

For each binding mode, the docked position of the isoindolinone scaffold was preserved and novel ligands were generated by the addition of either R^1 or R^2 substituents from a list of commercially available reagents. The interaction between the ligands and the MDM2 protein was explored using a simulated annealing optimization of an empirical scoring function using the program Skelgen.[37] Ligands able to form at least one H-bond

with MDM2. Both stereoisomers of these compounds were docked into the published MDM2 crystal structure 1YCR,[16] using the program easyDock.[34] As a result of the lipophilic properties of the compounds and the open shape and lipophilicity of the MDM2 binding site, a large number of possible docking solutions were identified. A single, high-scoring binding mode was chosen for both **5** and **7** from a large number of low-energy docking solutions. This was selected as the basis for the first

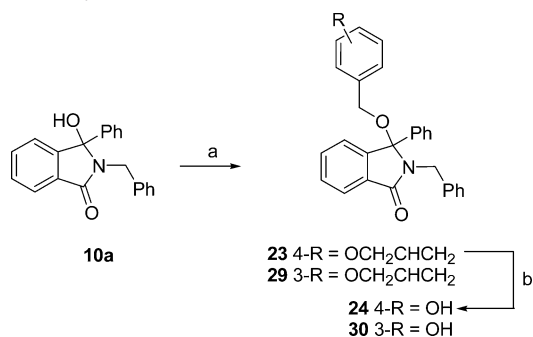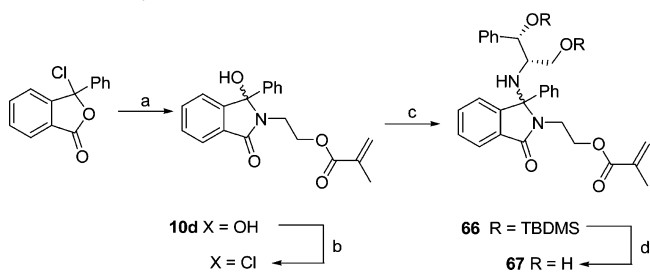**Scheme 4.** Synthesis of Substituted Isoindolinone **57**[a]

[a] Reagents and conditions: (a) $SOCl_2$, DMF, THF; (b) $TBDMSOC_4H_8NH_2$, THF; (c) $SOCl_2$, DMF, THF; (d) TBAF, THF; (e) $COCl_2$, DMSO, −78 °C; (f) MeOH, NH_4Cl.

Scheme 5. Synthesis of Substituted Isoindolinones **24** and **30**[a]

10a

23 4-R = OCH₂CHCH₂
29 3-R = OCH₂CHCH₂
24 4-R = OH
30 3-R = OH

[a] Reagents and conditions: (a) (i) SOCl₂, DMF, THF; (ii) 4-allyloxy-benzyl alcohol or 3-allyloxybenzyl alcohol, K₂CO₃, THF; (b) K₂CO₃, Pd(PPh₃)₄, MeOH.

Scheme 6. Synthesis of Substituted Isoindolinone **67**[a]

10d X = OH
X = Cl

66 R = TBDMS
67 R = H

[a] Reagents and conditions: (a) (i) SOCl₂, DMF, THF; (b) 2-aminoethyl methacrylate hydrochloride, Et₃N, THF; (b) SOCl₂, DMF, THF; (c) 2-(TBDMSO)-1-(TBDMSOmethyl)-2-phenylethylamine, Et₃N, DMF; (d) TBAF, THF.

Scheme 7. Synthesis of Substituted Isoindolinone **43**[a]
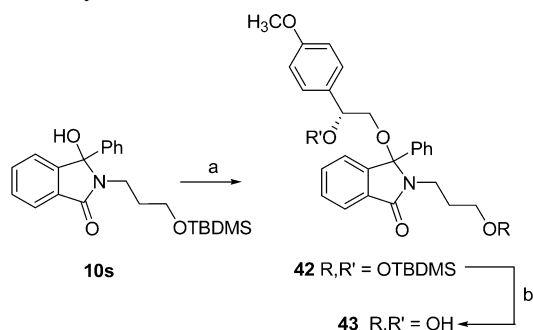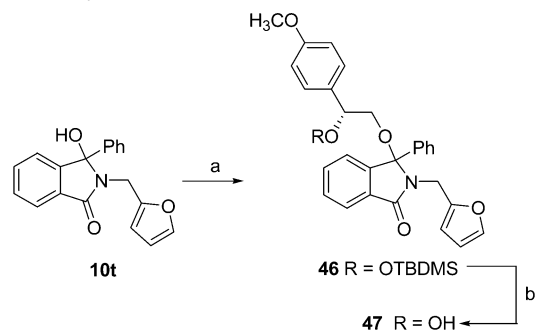

10s

42 R,R' = OTBDMS
43 R,R' = OH

[a] Reagents and conditions: (a) (i) SOCl₂, DMF, THF; (ii) (R)-2-(TBDMSO)-2-(4-methoxyphenyl)ethylamine, Et₃N, DMF; (b) TBAF, THF.

with target residues of MDM2 were selected as "virtual hits" and suggested for synthesis, and a set of 57 ligands were identified and suggested for synthesis.

Chemistry

Substituted isoindolinones were prepared according to Scheme 1. The appropriate benzoylbenzoic acids (**8**) were converted into the ψ-acid chlorides (**9**) under Vilsmeier conditions and condensed with the R¹-primary amines to give the 4-hydroxy-isoindolinones (**10**). The 4-hydroxy compounds (**10**) were converted into their respective chlorides (**11**) and, subsequently, reacted with appropriate alcohols in the presence of base (Et₃N or K₂CO₃) to give the final substituted isoindolinones (**13**, **19**–**22**, **25**, **26**, **31**–**40**, **44**, **45**, **48**–**51**, **64**, **65**, **68**–**73**, **75**, and **78**–**83**) as racemates (Scheme 1).[38]

The instability of the intermediate chlorides (**11**) to hydrolysis posed some difficulties in their efficient handling in a parallel synthesis approach. Consequently, we sought a stable intermediate that could be activated in situ. The activation of thioethers

Scheme 8. Synthesis of Substituted Isoindolinone **47**[a]

10t

46 R = OTBDMS
47 R = OH

[a] Reagents and conditions: (a) (i) SOCl₂, DMF, THF; (ii) (R)-2-(TBDMSO)-2-(4-methoxyphenyl)ethylamine, Et₃N, DMF; (b) TBAF, THF.

Scheme 9. Synthesis of Substituted Isoindolinone **65**[a]

10u R = H
X = OH
10v R = COCH₃
X = OH
X = Cl
R = COCH₃

65
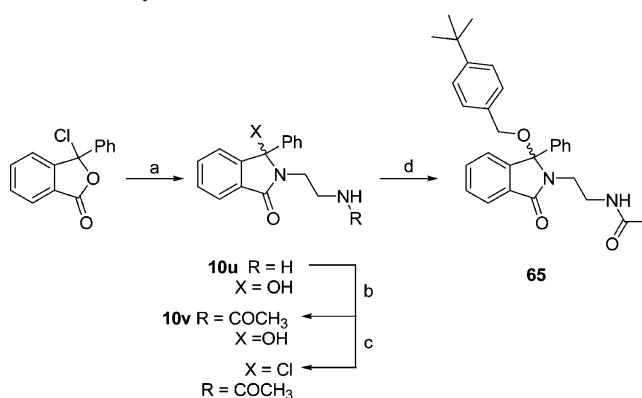
[a] Reagents and conditions: (a) ethylenediamine, THF; (b) Ac₂O, pyridine; (c) SOCl₂, DMF, THF; (d) 4-*tert*-butylbenzyl alcohol, Et₃N, THF.

Scheme 10. Synthesis of Substituted Isoindolinones **28** and **41**[a]

11a

27

28

41
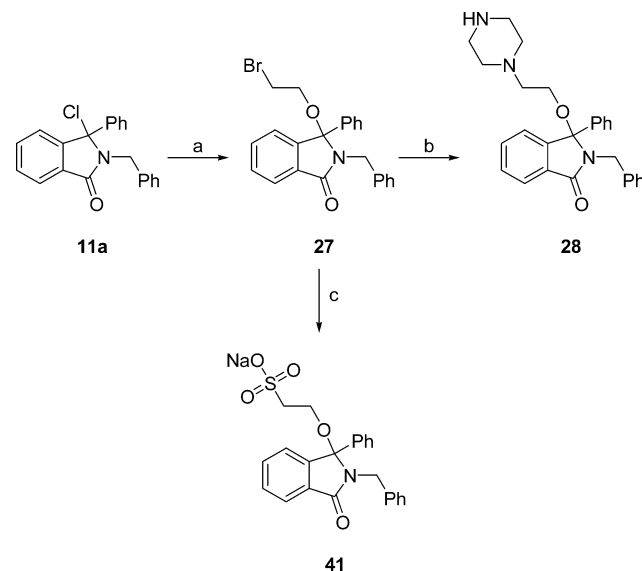
[a] Reagents and conditions: (a) 2-bromoethanol, THF; (b) piperazine, MeOH, reflux; (c) sodium sulfite, DME, water, reflux.

to nucleophilic displacement by oxidation is an established strategy in the synthesis of substituted pyrimidines, with *m*-chloroperbenzoic acid as oxidant.[39] To investigate this route, 4-hydroxyl compounds **10** were converted into the unstable chlorides (**11**) and trapped with benzylmercaptan to give the stable thioethers (**12a,b**). The oxidation of **12a** or **12b** using *m*CPBA was attempted, followed by displacement with an alcohol. However, this resulted in decomposition of the starting material, with no product identified by LC-MS or NMR in the crude reaction mixture. Successful activation of the thioethers

Scheme 11. Synthesis of Substituted Isoindolinones via a Directed *ortho*-Metalation Reaction[a]

10j,l X = OH   Y = O: **58-64, 84-87**
10m,n X = NH₂   Y = NH: **16,17**
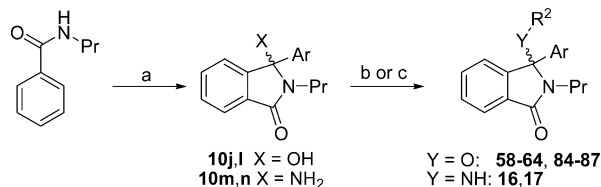
[a] Reagents and conditions: (a) *s*-BuLi, TMEDA, THF, −78 °C; (b) (i) SOCl₂, DMF, THF; (ii) R²OH, Et₃N, THF; (c) RCOCl, Et₃N, DCM.

12a and **12b** to nucleophilic displacement was achieved by treatment with *N*-iodosuccinimide (NIS) in the presence of catalytic camphorsulfonic acid (CSA).[40] The oxidized intermediates were reacted in situ with the appropriate R²-alcohol to give compounds **74**, **76**, and **77** (Scheme 2).

In selected cases, where the R¹-amine substituent contained additional nucleophilic amino or hydroxyl groups, a protecting group strategy was required. Similarly, isoindolinones **10q,r** were prepared using the required *tert*-butyldimethylsilyl-protected amino alcohols, which proved stable under the Vilsmeier conditions employed. Following appropriate substitution at C-3 to give **52** and **54**, deprotection with tetrabutyl-ammonium fluoride (TBAF) gave the alcohols **53** and **55**, respectively (Schemes 3 and 4). The alcohol **55** was used as the precursor to the dimethylacetal **57**. Oxidation of **55** under Swern conditions gave the aldehyde **56**, which was converted into the **57** under mild acidic conditions in methanol.

Protection was also required to ensure the correct regio-selectivity for R²-substitutions with multiple nucleophilic groups. The 3- and 4-hydroxybenzyl alcohol substituents were introduced as their allyl ethers giving **29** and **23**, respectively. Deprotection was effected under Pd(0) catalysis with methanol and potassium carbonate giving phenols **30** and **24**, respectively (Scheme 5). 2-Hydroxy-1-hydroxymethyl-2-phenylethylamine was introduced as its bis-*tert*-butyldimethylsilyl ether giving **67** following deprotection (Scheme 6). Similarly, silyl protection
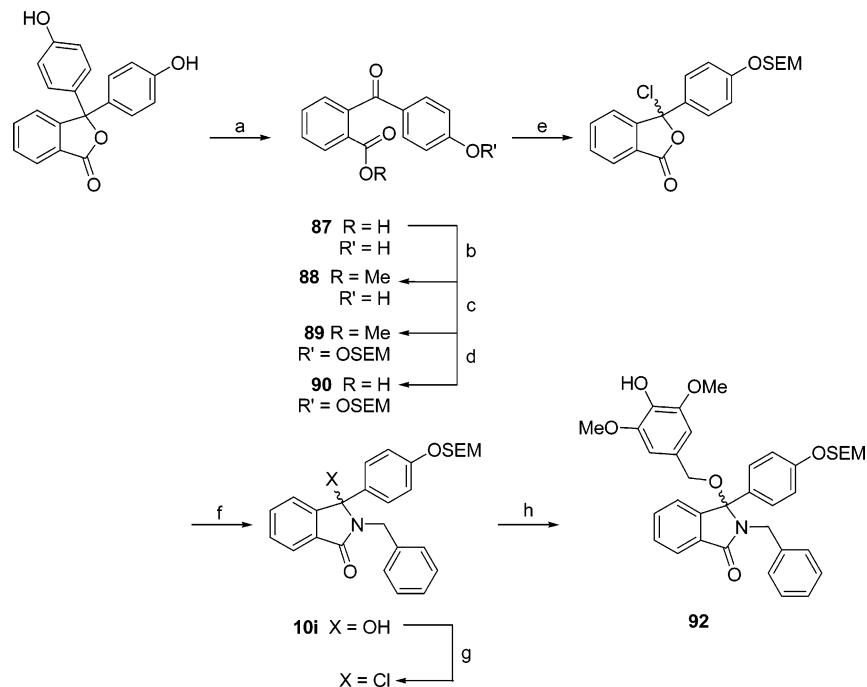
was required for both the 2-(3-hydroxypropyl) substituent and the secondary hydroxyl group of the 2-hydroxy-2-(4-methoxy-phenyl)ethanol used in the synthesis of **43** (Scheme 7). Silyl protection was also employed in the synthesis of **47** from 2-hydroxy-(4-methoxyphenyl)ethanol (Scheme 8).

The synthesis of 2-ethylacetamide derivatives could be achieved by direct synthesis, albeit in low yield. In the case of the *tert*-butylbenzyloxy derivative, ethane-1,2-diamine was reacted with the ψ-acid chloride to give the isoindolinone **10u**, which was acetylated to **10v** prior to conversion into the chloride and subsequent reaction to give **65** (Scheme 9).

Two isoindolinones were synthesized from the 2-bromoethoxy isoindolinone (**27**) as the common intermediate. Nucleophilic displacement of bromide with either piperazine or sulfite gave **28** and **41**, respectively (Scheme 10).

An alternative route to substituted 2-*n*-propyl isoindolinones proceeded by directed *ortho*-metalation of *n*-propylbenzamide and reaction with the appropriate benzoate ester or benzonitrile to give the hydroxyisoindolinone **10l** or aminoisoindolinones **10m,n**, respectively. The hydroxyisoindolinone **10l** was converted into the chloride and substituted with the appropriate alcohol or amine to give the desired isoindolinones **58**−**64** and **84**−**87**. Aminoisoindolinones **10m,n** were treated with the appropriate acid chloride to give the amides **16** and **17**, respectively (Scheme 11).

The silylethoxymethoxybenzoic acid (**92**) was prepared from phenolphthalein by hydrolysis to the benzoic acid (**88**),[41] which was esterified to **89** before conversion to the SEM ether **90** and saponification to **91**. The benzoic acid **91** was converted into the ψ-acid chloride and onto the hydroxyisoindolinone (**10i**). Isoindolinone **10i** was converted into the chloride and treated with syringic alcohol to give **92** (Scheme 12).

Results and Discussion

Structure−Activity Relationships for Inhibition of the MDM2−p53 Interaction. The virtual screening using multiple binding modes suggested a large set of novel ligands. A set of

Scheme 12. Synthesis of Substituted Isoindolinone **92**[a]

87 R = H   R' = H
88 R = Me   R' = H
89 R = Me   R' = OSEM
90 R = H   R' = OSEM

10i X = OH
X = Cl

92

[a] Reagents and conditions: (a) KOH, hydroxylamine hydrochloride, H₂O, 80 °C; (b) AcCl, MeOH; (c) Cs₂CO₃, SEMCl, CH₃CN; (d) TMSOK, DCM; (e) SOCl₂, DMF, THF; (f) BnNH₂, Et₃N, THF; (g) SOCl₂, DMF, THF; (h) syringic alcohol, THF.

Table 2. Inhibition of the MDM2−p53 Binding Interaction by Isoindolinones with R^1 and R^2 Reagents Selected from the Second Virtual Screen, Considering Multiple Binding Modes
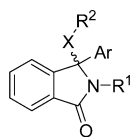
Compound	Ar	-R^1	-XR^2	ELISA IC$_{50}$ (µM)	Binding Mode
19	Ph			284 ± 19	01 Unique
20	Ph			393 ± 54	01
21	Ph			439 ± 35	01
22	Ph			78 ± 16	02 Unique
24	Ph			79 ± 11	02 Unique
25	Ph			311 ± 55	03 Unique
26	Ph			281 ± 70	03
28	Ph			315 ± 72	03
30	Ph			58 ± 14	05
31	Ph			206 ± 37	06 Unique
32	Ph			221 ± 25	06 Unique
33	Ph			214 ± 56	06
34	Ph			97 ± 30	06
35	Ph			96 ± 30	08
36	Ph			116 ± 20	09
37	Ph			243 ± 10	09
38	Ph			191 ± 45	09 Unique
39	Ph			232 ± 16	10
40	Ph			17.9 ± 0.3	10 Unique
41	Ph			345 ± 55	10
43	Ph			326 ± 64	10
44	Ph			490 ± 10	11 Unique
45	Ph			>500	11 Unique

Table 2 (Continued)

Compound	Ar	-R^1	-XR^2	ELISA IC$_{50}$ (µM)	Binding Mode
47	Ph	(2-furylmethyl)	(4-OMe phenyl, OH)	181 ± 46	12 Unique
48	Ph	(4-methoxybenzyl)	(propyl ether)	413 ± 54	19 Unique
49	Ph	(OMe, OH aryl)	(N-phenyl, CN)	88 ± 13	19
50	Ph	(OMe, OH aryl)	(NO$_2$ imidazole)	275 ± 14	19
51	Ph	(OMe, OH aryl)	(acetate ester)	380 ± 53	19
53	Ph	(OH)	(propyl ether)	>500	19 Unique
57	Ph	(OMe, OMe)	(propyl ether)	70 ± 6	19 Unique
58	4-tert-butylphenyl	(butyl)	(SO$_2$Me)	290 ± 40	15
59	4-tert-butylphenyl	(butyl)	(2-hydroxybenzamide)	70.1 ± 2.8	15 Unique
60	4-tert-butylphenyl	(butyl)	(nitro methylenedioxy)	70.2 ± 4.3	15
61	4-tert-butylphenyl	(butyl)	(4-hydroxyphenethyl)	69.7 ± 8.8	16
62	4-tert-butylphenyl	(butyl)	(imidazolidinone)	74.3 ± 3.1	16
63	4-tert-butylphenyl	(butyl)	(methylimidazole)	64.3 ± 7.7	16
64	4-OSEM-phenyl	(butyl)	(NO$_2$, NO$_2$, methyl aryl)	103 ± 44	21
65	Ph	(N-ethylacetamide)	(4-tert-butylbenzyl)	14.4 ± 0.3	06 Unique
67	Ph	(methacrylate ester)	(amino diol phenyl)	103 ± 43	03 Unique

43 compounds from this set were prepared, covering 14 of the 24 binding modes (BM01–BM24; Table 2). Where possible, substituents that only appeared in a single binding mode were chosen with the intention that a small number of preferred binding modes would be identified. Compounds with such substituents are labeled *unique* in Table 2. Of the 43 compounds evaluated, five displayed little or no inhibitory activity (**21**, **44**, **45**, **48**, and **53**; IC$_{50}$ > 400 µM). Approximately half of the group inhibited in the range 100–400 µM. Twelve compounds (**22**, **24**, **30**, **34**, **35**, **49**, **57**, and **59**–**63**) displayed similar activity (IC$_{50}$ = 50–100 µM) to the six seed compounds used in the binding mode study. Two compounds (**40** and **65**) displayed improved activity over the most potent seed compound **16**. Compounds displaying similar or improved activity were identified from a number of potential binding modes, suggesting that the isoindolinone may adopt different orientations within the MDM2 binding pocket depending on the R^1 and R^2 substituents. A number of binding modes suggested compounds with no significant activity (e.g., BM01, BM03, and BM11), and so, it may be reasonable to disregard these orientations. In contrast, two binding modes, BM06 and BM10, are of interest,

as they suggested the most active compounds **40** and **65**, respectively (Figure 1).

BM06 models the isoindolinone scaffold occupying the Trp23 binding pocket, the *N*-ethylacetamide group making a hydrogen bond to Gln72 in the region occupied by Phe19 of p53 and the *tert*-butylbenzyl group overlaying the surface of MDM2. In contrast, BM10 models the isoindolinone scaffold overlaying the surface of MDM2 with the Trp23 pocket occupied by the 3-phenyl group, the syringic alcohol substituent occupies the Leu26 pocket and makes a hydrogen bond to Tyr100, and the *N*-benzyl substituent occupies the Phe19 pocket. In comparison, the X-ray structures of Nutlin-2 (**3a**) and the **4**, both the Leu26 and Trp23 pockets are occupied by 4-bromophenyl and 4-chloro-phenyl residues, respectively, and the Phe19 pocket is occupied by a combination of the 2-ethoxy-4-methoxyphenyl and the *N*-hydroxyethylpiperazine residues for **3a** and the 7-iodobenzo-diazepinedione ring of **4**.

Bearing in mind that these compounds were uniquely identified for specific binding modes it is tempting to consider these binding modes as possible experimental solutions. The SARs indicate that multiple binding modes are likely to exist
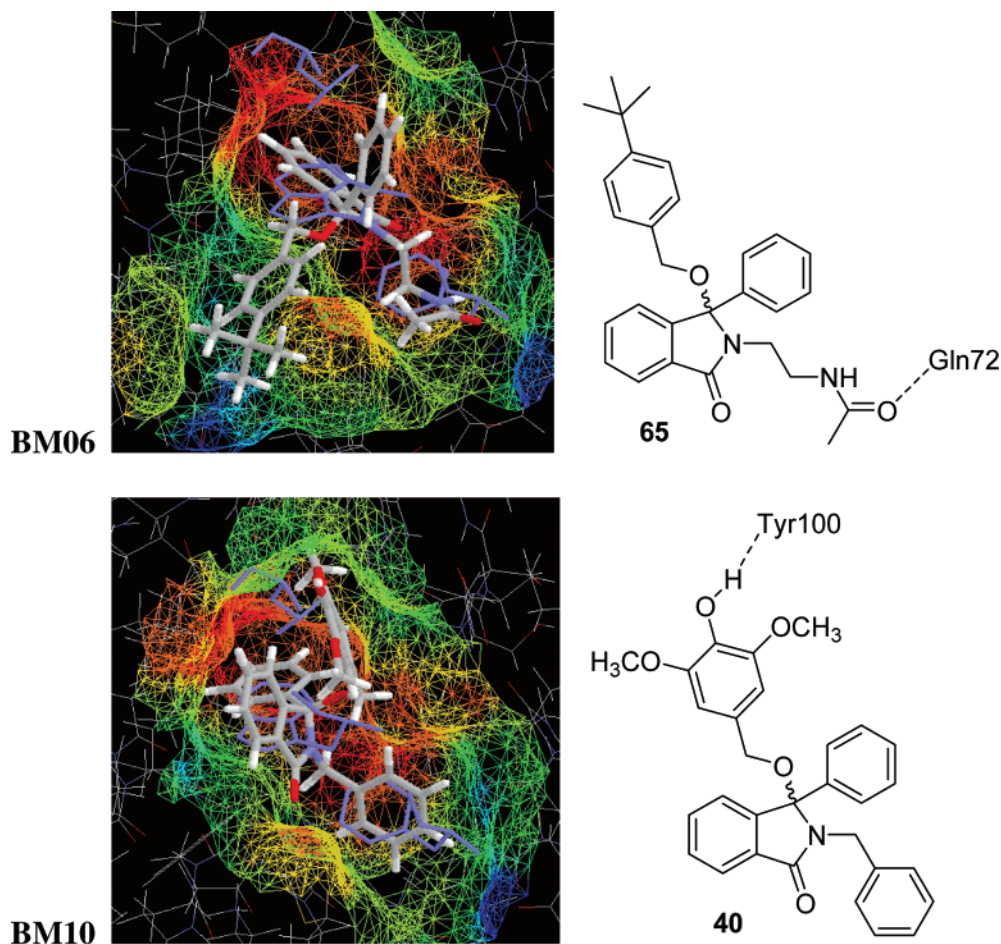
Figure 1. Compounds **65** and **40** docked into MDM2 structure (1YCR) showing binding modes BM06 and BM10, respectively, and cartoons indicating the predicted hydrogen bond; p53 residues (purple) are included for reference.
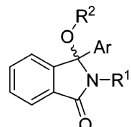
for the isoindolinone compounds. The fact that binding modes BM06 and BM10 also suggested a number of compounds with poorer activity than the seed compounds might not necessarily indicate a flaw in the binding mode prediction, but perhaps instead that those reagents were false positives in the virtual screen. Determination of the structure of the isoindolinone–MDM2 complex is in progress and will provide experimental validation of the binding modes and shed further light onto the results of the virtual screening.

In the absence of a confirmed binding mode for the iso-indolinone inhibitors, we decided to employ a combinatorial approach to optimize the activity of this series of compounds. Based on the experimental data (Tables 1–2), the most favorable substituents at each of the three positions of variation on the isoindolinone template were identified. At the R^1 position benzyl, *n*-propyl, and 2-acetamidoethyl were selected. At the R^2 position phenyl, 4-chlorophenyl, and 4-trimethylsilyl-ethoxymethoxyphenyl (4-SEMOPh) were chosen as the most favorable aromatic substituents, and 4-*tert*-butylbenzoxy, 3,5-dimethoxy-4-hydroxybenzoxy, 3-hydroxypropoxy, and 2-(2-pyridyl)ethoxy were selected as the ether substituents conferring the best activity. An array of 36 isoindolinones of covering every possible combination of substituent was designed. For certain substituents, where the preliminary biological activity was discouraging and the synthesis lengthy or problematic, the synthesis of every combination was not attempted. A total of 24 array compounds were synthesized and assayed (Table 3).

The results shown in Table 3 indicate the following: **68**–**70**, **72**, **73**, **78**, **84**–**87**, and **92** displayed lower potency than their parents; **13**, **71**, **74**, **75**, and **81**–**83** displayed comparable

activity with the parent compounds; and **40**, **65**, **76**, **77**, **79**, and **80** were the most potent in the group. A comparison of the results between the R^2 substituents reveals that the 4-trimethyl-silylethoxymethoxyphenyl was not favorable in all cases. The modest activity of some compounds bearing the 4-SEMOPh may be due to nonspecific hydrophobic interactions between the bulky lipophilic substituent and the largely hydrophobic binding pocket of MDM2. Comparison between the R^2-phenyl and 4-chlorophenyl series reveals contrasting SAR for the *N*-benzyl and *N*-*n*-propyl substituents. In the *N*-*n*-propyl series, the 4-chlorophenyl substituent confers improved activity over the parent phenyl in every case. The effect is most striking between the 3-hydroxypropoxy derivative **72**, which is essentially inactive, and **80** (IC$_{50}$ = 16.4 μM). In the case of the syringic alcohol derivatives **71** and **79**, a 16-fold gain in activity is observed for the 4-chloro compound. In contrast, in the *N*-benzyl series, the 4-chloro substituent is favorable in the case of the 3-hydroxypropoxy and 2-(2-pyridyl)ethoxy derivatives (**68** and **69** vs **76** and **77**) but unfavorable for the syringic alcohol substituent (**40** vs **75**). For the one comparable example in the *N*-(2-acetamidoethyl) series the 4-chloro substituent is not favored. These results suggest that the *N*-benzyl and *N*-*n*-propyl isoindolinones bind to MDM2 in different orientations, resulting in different SARs. The most potent isoindolinone identified from the array is **79** (NU8231; IC$_{50}$ = 5.3 $\pm$ 0.9), which shows a 4-fold improvement in potency over the parent **40**.

The presence of 4-haloaromatic substituents in potent MDM2–p53 inhibitors demonstrates that these substituents produce favorable binding interactions in both the Trp23 and the Leu26 binding pockets.[23–26] The gains in potency seen for the 4-chloro-

Table 3. Inhibition of the MDM2−p53 Binding Interaction by Isoindolinones Members of the Combinatorial Array

Compound	Ar	R^1	R^2	IC$_{50}$ (μM)
13	Ph	benzyl	*p*-*t*-Bu-phenyl	92 ± 11
40	Ph	benzyl	2-OMe,4-OH,6-OMe-phenyl	17.9 ± 0.3
68	Ph	benzyl	propyl-OH	245
69	Ph	benzyl	pyridinyl	206 ± 30
70	Ph	*n*-Pr	*p*-*t*-Bu-phenyl	>500
71	Ph	*n*-Pr	2-OMe,4-OH,6-OMe-phenyl	82 ± 8
72	Ph	*n*-Pr	propyl-OH	>500
73	Ph	*n*-Pr	pyridinyl	100 ± 14
65	Ph	CH$_2$CH$_2$NHC(O)CH$_3$	*p*-*t*-Bu-phenyl	14 ± 0.3
74	*p*-Cl-phenyl	benzyl	*p*-*t*-Bu-phenyl	99 ± 18
75	*p*-Cl-phenyl	benzyl	2-OMe,4-OH,6-OMe-phenyl	42 ± 8
76	*p*-Cl-phenyl	benzyl	propyl-OH	15.9 ± 0.8
77	*p*-Cl-phenyl	benzyl	pyridinyl	26.2 ± 4.2
78	*p*-Cl-phenyl	*n*-Pr	*p*-*t*-Bu-phenyl	187 ± 38
79	*p*-Cl-phenyl	*n*-Pr	2-OMe,4-OH,6-OMe-phenyl	5.3 ± 0.9
80	*p*-Cl-phenyl	*n*-Pr	propyl-OH	16.4 ± 1.6
81	*p*-Cl-phenyl	*n*-Pr	pyridinyl	57 ± 6
82	*p*-Cl-phenyl	CH$_2$CH$_2$NHC(O)CH$_3$	*p*-*t*-Bu-phenyl	91.4 ± 0.4
83	*p*-Cl-phenyl	CH$_2$CH$_2$NHC(O)CH$_3$	2-OMe,4-OH,6-OMe-phenyl	76 ± 4
84	*p*-OSEM-phenyl	*n*-Pr	*p*-*t*-Bu-phenyl	464 ± 31
85	*p*-OSEM-phenyl	*n*-Pr	2-OMe,4-OH,6-OMe-phenyl	118 ± 24
86	*p*-OSEM-phenyl	*n*-Pr	propyl-OH	476 ± 24
87	*p*-OSEM-phenyl	*n*-Pr	pyridinyl	312 ± 22
92	*p*-OSEM-phenyl	benzyl	2-OMe,4-OH,6-OMe-phenyl	257 ± 34

phenyl-substituted isoindolinones series are consistent with these observations and with the predicted binding mode BM10.
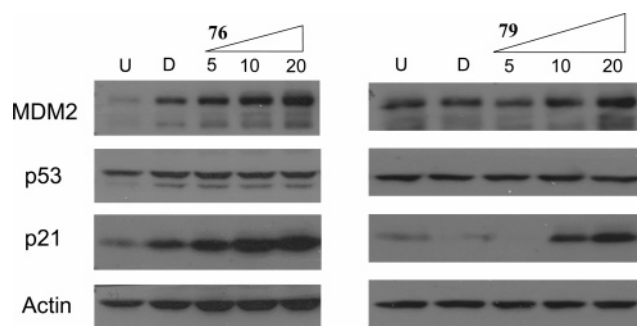
Figure 2. Western blot analysis of SJSA cells treated with increasing concentrations (5−20 μM) of compounds **76** and **79**, showing the induction of dose-dependent increases in MDM2 and p21 protein levels.
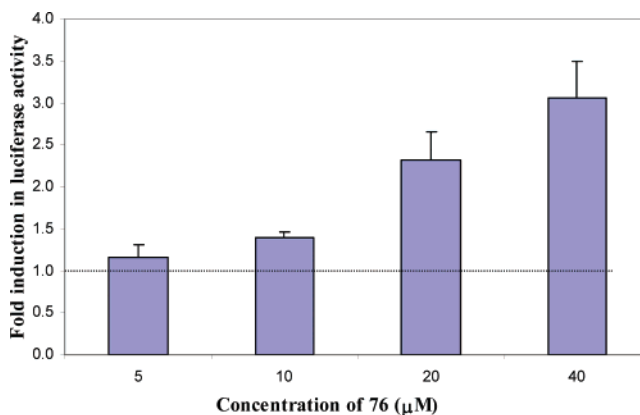
Figure 3. Change in p53-dependent luciferase activity in SJSA cells treated with increasing concentrations (5−40 μM) of **76** for 6 h. The bars represent the mean and standard errors for three independent experiments. Increases that were significantly higher (p < 0.05; two-tailed t-test) than the DMSO control level (broken line) are marked by an asterisk.

Cell Biology. The most potent compounds identified were selected for further evaluation to ascertain whether they had effects on intact cells that were consistent with inhibition of MDM2−p53 binding. Compounds **76** and **79** showed significant biological activity. SJSA cells, in which the MDM2 gene is amplified, were treated with increasing concentrations (5, 10, and 20 μM) of **76** and **79**. Cells were lysed at 6 h and protein extracts were analyzed by western immunoblotting for p53, p21^{WAF1}, and actin (Figure 1). Compounds **76** and **79** produced a dose-dependent increase in MDM2 and p21, consistent with the release of p53 transcriptional activity. Surprisingly, the accumulation of p53 protein levels was not observed in the SJSA cells under these conditions. To test for further evidence of increased p53 transcriptional activity in response to treatment with the compounds, a luciferase-based reporter gene assay was used. This assay again showed the induction of a dose-dependent increase in p53 transcriptional activity for both **76** (Figures 2 and 3) and **79** (data not shown).

Conclusions

We have demonstrated the utility of docking and in silico combinatorial methods in the optimization of a series of inhibitors of the MDM2−p53 interaction based on an iso-indolinone scaffold. We consider that the isoindolinones presented are an interesting addition to the small-molecule inhibitors of the MDM2−p53 protein−protein interaction. Further optimization of this class of compounds is in progress.

Experimental Section

Computational Chemistry. The computational methods used for this work include binding-mode prediction through docking and virtual screening of substituents for the isoindolinone scaffold. For both purposes, the crystal structure 1YCR[16] of MDM2 was prepared by removing the p53 peptide and adding hydrogen atoms in InsightII/Discover3 (Accelrys, Inc., San Diego, CA) at pH 7.0. Their positions were subject to 500 iterations of steepest descent minimization, followed by 500 steps of conjugate gradient minimization using the CFF force field.[42] All nonhydrogen atoms were held rigid during these minimizations.

Docking studies were carried out using the programs easyDock[34] and GOLD.[36] The selection of binding modes from the large pool of solutions for the second round of docking was performed according to a protocol described previously.[35] In brief, the ligand binding modes were ordered according to their binding energies. Then, starting from the lowest-energy solution, the rmsd of each pose with respect to all the previous lower-energy poses was computed. If the rmsd was higher than a given threshold (1.5 Å), then that pose was added to a list of distinct solutions. The result of this procedure was a list of distinct ligand-binding mode poses that had rmsds between one another of more than the predefined threshold. The number of binding modes selected to be used in the second round of virtual screening was set to 24. This number was based on the fact that six compounds were used for the docking study, each of these with one stereocenter on the isoindolinone scaffold, and that two different docking programs were used.

Reagents derived from primary amines (R^1), acid chlorides (R^2), and primary alcohols (R^2) were extracted from the Daylight Available Chemicals Directory (ACD; Daylight Chemical Information Systems, Inc., CA). Reagents containing atoms other than C, O, N, S, Na, Ca, K, or halogens were removed from the set, as were molecules containing chains of more than five sequential carbon atoms, azides, aldehydes, and hydrazones, and molecules with MW > 350. For each reagent, the physiologically relevant protonation states were selected.

The de novo drug design program Skelgen was used for the virtual screen. A brief discussion of the Skelgen algorithm is given below, and further details of the principles involved as well as practical applications of the method can be found in previous publications.[37,43–45] Skelgen takes as input the three-dimensional coordinates of the protein, a rectangular box that defines the binding site pocket, and a predefined set of fragments. The algorithm invokes a simulated annealing procedure to minimize a function that assesses the suitability of molecular structures within the active site box. In this process, a set of initial fragments are randomly selected and connected together. The putative ligand is then altered by several transitions, which include rigid-body displacements, conformational changes, and fragment addition, deletion, and replacement. The transition type is randomly chosen, and at each step the value of the objective function is determined. The modified structure is accepted or rejected on the basis of the Metropolis condition, $p = \exp(\Delta F/T)$, where ΔF represents the change in value of the objective function resulting from the transition, T is the temperature, which is lowered during the annealing procedure, and p is the probability of acceptance of the transition. The length of each Skelgen annealing run is defined by the number of transitions at each temperature setting, termed the Markov chain length, and by the number of Markov chains as the temperature is depressed. The algorithm generates one structure for each run, and as a result of the stochastic nature of the simulation, different random starts can lead to different solutions.

In this work, Skelgen was used in reagent screening mode, such that each reagent in our data set was attached to a fixed isoindolinone core and individually subject to a Skelgen simulated annealing run, and thus, transition types for fragment addition, deletion, and replacement were switched off, as were the translation and rotation of the whole ligand. Only transition types for conformational changes of the attached reagent were retained. The objective function comprises several terms, which are conferred a zero value when the appropriate constraints are satisfied and conferred a positive value otherwise. The constraints used in this work included intramolecular ligand van der Waals clashes and intermolecular ligand−protein van der Waals clashes, both according to the Bondi set.[46] A reagent was deemed to be successful in the virtual screen, yielding a "hit", if it was able to form at least one H-bond with the following H-bond anchoring points of MDM2: Leu 54 O, Phe 55 O, Gln 59 NE2, Gln 72 O and OE1, Val 93 O, His 96 ND1, and Tyr 100 OH. The isoindolinone scaffold was held rigid during the screen. For ranking purposes, a scoring function very similar to Böhm's empirical scoring function was used as a measure of ligand−protein interactions.[47,48] The scoring function is knowledge-based and includes H bonds, ionic interactions, lipophilic protein−ligand contacts, and the number of rotatable bonds in the ligand.

Synthesis. General Procedure A: Synthesis of 3-Hydroxy-isoindolin-1-ones. To a solution of the appropriate 2-benzoylbenzoic acid (1.0 equiv) in THF was added thionyl chloride (2.2 equiv) and DMF (3 drops). The mixture was stirred at room temperature 16 h and then concentrated in vacuo to give a clear oil. The residues were dissolved in THF (10 mL), the appropriate primary amine (1.0 equiv) and triethylamine (2.2 equiv.) were added, and the mixture was stirred at room temperature for 16 h. The mixture was either filtered and submitted to extraction with EtOAc (15 mL), sodium bicarbonate (20 mL), and water (15 mL) or treated immediately with EtOAc (15 mL), saturated sodium bicarbonate (15 mL), and water (15 mL). The organic layers were combined, dried (Na_2SO_4), and concentrated in vacuo. Chromatography (EtOAc, petrol 1:4) or crystallization, with a minimum of EtOAc and an excess of petrol, gave the desired product.

General Procedure B: 3-Alkoxy-2,3-dihydroisoindol-1-ones. To a solution of **11a** (0.51 g, 1.50 mmol) in THF (7 mL) was added the appropriate alcohol (3.0 or 4.0 mol equiv). The reactions were stirred at room temperature for 72 h, unless stated otherwise, and then concentrated in vacuo. The residue was dissolved in EtOAc (20 mL) and washed with water (3 × 10 mL). The organic layer was dried ($MgSO_4$) and concentrated in vacuo to give the crude 3-alkoxy-2,3-dihydroisoindol-1-one.

General Procedure C: 3-Alkoxy-2,3-dihydroisoindol-1-ones (NIS Method). The appropriate 3-benzylsulfanylisoindol-1-one (1 mol equiv) in THF (4 mL) was added to a solution of NIS (1.1 mol equiv), CSA (0.1 mol equiv), and the appropriate alcohol (2.2 mol equiv) in THF (3 mL). The reaction was stirred in the dark for 4 h at room temperature and then concentrated in vacuo. The residue was dissolved in EtOAc (30 mL) and washed with aqueous sodium thiosulfate (2 × 30 mL). The organic layer was collected, dried (Na_2SO_4), and concentrated in vacuo to give the 3-alkoxy-isoindol-1-one.

2-Benzyl-3-(4-chlorophenyl)-3-(3-hydroxypropoxy)-2,3-dihydroisoindol-1-one (76). General Procedure C. 12b (0.50 g, 1.10 mmol) in THF (4 mL), NIS (0.27 g, 1.21 mmol), CSA (0.03 g), and propane-1,3-diol (0.17 mL, 2.35 mmol) in THF (3 mL) was purified by chromatography (silica gel, 40:60 EtOAc/petrol), followed by recrystallization (EtOAc, petroleum ether) to give **76** as a white solid (0.17 g, 0.42 mmol, 39%); mp 149−151 °C. IR (Diamond ATR) v_{max} (cm^{-1}): 3431 (OH), 1669 (CO), 1426, 1399, 1359, 1066, 1012, 818, 766, 700. ^{1}H NMR (300 MHz, CDCl$_3$) δ 1.21−1.43 (2H, m, OCH$_2$C*H*$_2$CH$_2$OH), 1.53 (s, CH$_2$O*H*, ex), 2.69−2.74 (2H, m, C*H*$_2$OH), 3.40−3.44 (2H, m, OC*H*$_2$CH$_2$CH$_2$O), 3.89−3.94 (1H, d, J = 14.5 Hz, NC*H*$_2$), 4.69−4.74 (1H, d, J = 14.5 Hz, NC*H*$_2$), 7.01−7.10 (1H, m, Ar-*H*), 7.12−7.23 (9H, m, Ar-*H*), 7.40−7.46 (2H, m, Ar-*H*), 7.82−7.88 (1H, m, isoindolinone-*H*). ^{13}C NMR (300 MHz, CDCl$_3$) δ 32.02 (OCH$_2$*C*H$_2$CH$_2$OH), 43.35 (N*C*H$_2$), 60.70 and 60.83 (O*C*H$_2$CH$_2$*C*H$_2$OH), 95.38 (*C*-3), 123.11, 124.04, 127.58, 128.16, 128.53, 128.96, 129.55, 130.15, 131.81, 133.08, 134.73, 137.50, 137.89, 145.51, 165.76 (*C*-1). LC-MS (ESI+) *m/z* 332, 334, 408 [M + H]$^+$. Anal. (C$_{24}$H$_{22}$ClNO$_3$) C, H, N.

General Procedure D: Synthesis of Isoindolin-1-ones Derivatives with R4 Amino Substitutions. A solution of the appropriate 3-hydroxyisoindolinone **10** (1.0 equiv) in THF (10 mL) was treated with a solution of thionyl chloride (2.2 equiv) and a catalytic amount of DMF. The mixture was stirred 16 h and then concentrated in

vacuo. The residues were dissolved in either DMF (10 mL) or acetonitrile (10 mL), as appropriate, and treated with the appropriate primary amine (1.1 equiv) and either anhydrous potassium carbonate (2.2 equiv) or triethylamine (2.2 equiv). The mixture was stirred at room temperature under a nitrogen atmosphere, (EtOAc/petrol, 3:2). After 20 h, the solvent was removed in vacuo. The crude product was extracted with EtOAc (15 mL) and water (20 mL). The organic layers were combined, dried (Na_2SO_4), and concentrated in vacuo. Purification was done by flash chromatography (EtOAc/petrol, 1:4) and by recrystallization from suitable solvents.

General Procedure E: Synthesis of Isoindolin-1-ones Derivatives with R4 Alkoxy Substitution. A solution of the appropriate 3-hydroxyisoindolinone **10** (1.0 equiv) in THF (10 mL) was treated with a solution of thionyl chloride (2.2 equiv) and a catalytic amount of DMF. After 16 h, the mixture was concentrated in vacuo. The residues were dissolved in either DMF (5−10 mL) or THF (5−10 mL), as appropriate, and treated with the appropriate primary alcohol (1.1 equiv or 2.2 equiv) with or without triethylamine (2.2 equiv). The reaction mixture was stirred at room temperature for 20 h, and the workup was performed as for general procedure D.

3-(4-Chlorophenyl)-3-(4-hydroxy-3,5-dimethoxybenzyloxy)-2-propyl-2,3-dihydroisoindol-1-one (79). General Procedure E: 10k (250 mg, 0.82 mmol) and syringic alcohol (331 mg, 1.80 mmol) were purified by chromatography (45% EtOAc, petroleum ether) and HPLC (Genesis C18; H_2O/CH_3CN, 270 nm) to give **79** as a light red oil (180 mg, 0.38 mmol, 46%). λ_{max} (CH_3OH)/nm 209, Abs 0.550. IR: 3360, 2933, 1692, 1604, 1504, 1450 cm^{-1}. ^{1}H NMR (300 MHz, CDCl$_3$) δ 0.74 (t, 3H, $J = 7.4$ Hz, CH$_2$CH$_2$CH_3), 1.31 (m, 1H, NCH$_2$CH_2), 1.44 (m, 1H, NCH$_2$CH_2), 3.03 (m, 1H, NCH$_2$), 3.23, (m, 1H, NCH$_2$), 3.79 (s, 6H, OMe), 3.84 (d, 1H, $J = 11.1$ Hz, OCH$_2$), 4.08 (d, 1H, $J = 11.2$ Hz, OCH$_2$), 5.45 (s, 1H, OH), 6.38 (s, 2H, Ar-H), 7.05 (m, 1H, Ar-H), 7.22 (d, 2H, $J = 8.9$ Hz, Ar-H), 7.28 (d, 2H, $J = 8.7$ Hz, Ar-H), 7.42 (m, 2H, Ar-H), 7.83 (m, 1H, Ar-H). ^{13}C NMR (75 MHz, CDCl$_3$) δ 12.1, 22.1, 41.9, 56.7, 65.6, 95.1, 104.8, 123.5, 123.8, 128.2, 128.7, 129.1, 130.2, 132.3, 132.8, 134.7, 134.8, 138, 145.5, 147.3, 168.6. LC/MS (ESI+) m/z 302.1, 489.9, 500. Anal. ($C_{26}H_{26}ClNO_5$·0.1$C_4H_8O_2$) C, H, N.

MDM2-p53 interaction using a 96-well plate binding assay (ELISA). The 96-well black and white high binding luminometry isoplates (Wallac, Cat N^0 140−155) were coated by overnight incubation at 35 °C with 200 μL per well of 5 μg mL^{-1} streptavidin (Chemicon International) in coating buffer (0.1 M Na$_2$HPO$_4$·2H$_2$O; 0.1 M citric acid; pH 5.0). The plates were washed five times in 1× dissociation enhanced lanthanide fluorescence immunoassay (DELFIA) buffer (Wallac) and then incubated for 3 h at room temperature with saturation buffer (0.3 M D-sorbitol; 50 mM Tris; 150 mM NaCl; 0.1% BSA; 0.05% sodium azide; pH 7.0) to block nonspecific protein binding sites on the plate. After removal of the buffer from the plates, they were allowed to dry in a sterile laminar air flow hood at room temperature before incubation for 1 h at 4 °C with 200 μL per well of 100 μg mL^{-1} biotinylated IP3 peptide (b-IP3: Ac-Met-Pro-Arg-Phe^{19}-Met-Asp-Tyr-Trp-Glu-Gly-Leu^{26}-Asn-NH$_2$)[17] dissolved in 0.05% DMSO−PBS, pH 7.4 buffer. After washing the wells three times with PBS, the plates were ready to use for MDM2 binding.

For initial testing, the compounds and controls were plated out in triplicate into clear 96-well plates (Nunc) in 10-μL aliquots to give final concentrations of 500 μM, 100 μM, and 20 μM in the assay. Control samples consisted of 5% DMSO carrier alone as a negative control and 100 nM active peptide (AP-B: Ac-Phe^{19}-Met-Aib-Pmp-6-Cl-Trp-Glu-Ac$_3$-Leu^{26}-NH$_2$) as a positive control peptide antagonist of the MDM2−p53 interaction (IC$_{50}$ = 5 nM).[18] Compounds and controls aliquoted in 96-well plates were pre-incubated at 20 °C for 20 min with 190 μL aliquots of optimized concentrations of in vitro translated MDM2, before transfer of the MDM2-compound mixture to the b-IP3 streptavidin plates, and incubation at 4 °C for 90 min. After washing three times with PBS to remove unbound MDM2, each well was incubated at 20 °C for 1 h with a TBS-Tween (50 mM Tris pH 7.5; 150 mM NaCl; 0.05% Tween 20 nonionic detergent) buffered solution of primary mouse monoclonal anti-MDM2 antibody (Ab-5, Calbiochem, used at a 1/200 dilution), then washed three times with TBS-Tween before incubation for 45 min at 20 °C with a goat-anti-mouse horseradish peroxidase (HRP) conjugated secondary antibody (Dako, used at 1/2000). The unbound secondary antibody was removed by washing three times with TBS-Tween. The bound HRP activity was measured by enhanced chemiluminescence (ECL, Amersham Biosciences) using the oxidation of the diacylhydrazide substrate, luminol, to generate a quantifiable light signal. The luminol substrate together with enhancer was automatically injected into each well and the relative luminescence units (RLU) measured over a 30 s interval using a Berthold MicroLumat-Plus LB 96 V microplate luminometer. The percentage MDM2 inhibition at a given concentration is calculated as the (RLU detected in the compound treated sample ÷ RLU of DMSO controls) × 100. The IC$_{50}$ was calculated using a plot of % MDM2 inhibition versus concentration and is the average of three independent experiments. The results (mean ± S.D.) are presented in Table 1.

Cell-Based Assays. Western Blot Analysis. SJSA cells were treated for 6 h with 5, 10, and 20 μM of compounds **76** and **79** in 1% DMSO. The cells together with 1% DMSO only controls were washed with ice-cold phosphate buffered saline (PBS) and protein extracts prepared by lysing the cells in SDS buffer (62.5 mM Tris pH 6.8; 2% sodium dodecyl sulfate (SDS); 10% glycerol) with sonication for 2 × 5 s (Soniprep 150ME) to break down high molecular weight DNA and reduce the viscosity of the samples. The protein concentration of the samples was estimated using the Pierce BCA assay system (Pierce, Rockford, IL) and 50 μg aliquots of protein analyzed using standard SDS-polyacrylamide gel electrophoresis (SDS-PAGE) and western immunoblotting procedures. β-Mercaptoethanol (5%) and bromophenol blue (0.05%) were added and the samples, which were then boiled for 5 min, followed by brief centrifugation, before loading onto a precast 4−20% gradient Tris-glycine buffered SDS-polyacrylamide gel (Invitrogen). Molecular weight standards (SeeBlue, Invitrogen) were included on every gel, and electrophoresis was carried out in a Novex XL tank (Invitrogen) at 180 V for 90 min. The separated proteins were transferred electrophoretically overnight from the gel onto a Hybond C nitrocellulose membrane (Amersham) using a BioRad electrophoresis tank and 25 mM Tris, 190 mM glycine, and 20% methanol transfer buffer at 30 V. Primary antibodies used for immunodetection of the transferred proteins were: mouse monoclonal NCL-p53DO-7 (Novocastra) at 1:1000; MDM2 (Ab-1, clone IF2; Oncogene) at 1:500; WAF1 (Ab-1, clone 4D10; Oncogene) at 1:100; Actin (AC40; Sigma) at 1:1000. The secondary antibody used was peroxidase conjugated, affinity purified, goat anti-mouse (Dako) at 1:1000. Protein detection and visualization was performed by ECL (Amersham) with light detection by exposure to blue-sensitive autoradiography film (Super RX, Fuji).

Results of the analysis by western immunoblotting for p53, p21^{WAF1}, and actin are shown in Figure 1. A dose-dependent increase in MDM2 and p21^{WAF1} was observed in MDM2 amplified SJSA cells treated with compounds **76** and **79**, consistent with the release of transcriptionally active p53. No change was observed for p53 protein levels, although there was clear evidence of increased MDM2 and p21^{WAF1} expression.

p53-Dependent Reporter Gene Assay. The reporter gene assay used in this investigation involved the transient transfection of a plasmid luciferase reporter gene construct, pLubP2, which was made from a pGL3 plasmid (Invitrogen) into which a luciferase gene had been introduced downstream of the p53 responsive MDM2 P2 promoter.[49] The introduction of this plasmid into cells results in the expression of luciferase in a p53-dependent manner and, hence, an increase in the transcriptional activity of p53 is reflected in increased levels of luciferase. SJSA cells were seeded into 96-well clear bottom luminometer plates (Wallac) in RPMI medium (GIBCO) supplemented with 5% fetal bovine serum and allowed to attach overnight. Plasmid transfection was carried out using the FuGENE 6 transfection reagent (Roche Molecular Biochemicals). Each 25 μL transfection volume per well included 30 ng of the pLubP2 reporter plasmid or pGL3-basic empty vector as a negative control and 5 ng of pCMVβ-galactosidase (Stratagene) as a

Hardcastle et al.

transfection efficiency control per well, together with 0.2 μL of FuGENE 6, and the volume made up to 25 μL with serum-free medium.

Following 24 h transfection, the cells were treated with the MDM2 inhibitors, which were made up in cell culture medium to the appropriate concentration from concentrated stocks dissolved in DMSO. Five replicate wells were used for each inhibitor concentration. In addition, DMSO controls and untreated wells were included. Following the incubation period with the inhibitors, the 96-well plates were checked under a light microscope for possible lifting of cells. All the experiments carried out resulted in no detectable cell lifting. The medium from the wells was gently aspirated, and 25 μL of lysis buffer (Applied Biosystems) was added into each well. The plate was then shaken on a rocker for 5 min and stored at -20 °C until the luminometry was carried out. Luciferase and β-galactosidase activities were measured using a dual light chemiluminescence detection kit (Applied Biosystems) and a luminometer (LB 96 V, EG&G Berthold) to quantify the light emission. Normalized luciferase activity levels are calculated as a ratio of luciferase/β-galactosidase and fold-induction with the compounds calculated relative to the background with DMSO solvent control alone.

Supporting Information Available: Additional details of the first round of virtual screening, experimental details and analytical data for all compounds and intermediates, and a table of combustion analysis data. This material is available free of charge via the Internet at http://pubs.acs.org.

References

(1) Lane, D. P. Cancer. p53, guardian of the genome. *Nature* **1992**, *358*, 15−16.

(2) Vousden, K. H.; Lu, X. Live or let die: the cell's response to p53. *Nat. Rev. Cancer* **2002**, *2*, 594−604.

(3) Momand, J.; Zambetti, G. P.; Olson, D. C.; George, D.; Levine, A. The *mdm-2* oncogene product forms a complex with p53 protein and inhibits p53-mediated transactivation. *Cell* **1992**, *69*, 1237−1245.

(4) Fuchs, S. Y.; Adler, V.; Buschmann, T.; Wu, X. W.; Ronai, Z. Mdm2 association with p53 targets its ubiquitination. *Oncogene* **1998**, *17*, 2543−2547.

(5) Oliner, J. D.; Kinzler, K. W.; Meltzer, P. S.; George, D. L.; Vogelstein, B. Amplification of a gene encoding a p53-associated protein in human sarcomas. *Nature* **1992**, *358*, 80−83.

(6) Chene, P. Inhibiting the p53−MDM2 interaction: An important target for cancer therapy. *Nat. Rev. Cancer* **2003**, *3*, 102−109.

(7) Cochran, A. G. Antagonists of protein−protein interactions. *Chem. Biol.* **2000**, *7*, R85−R94.

(8) Cochran, A. G. Protein−protein interfaces: mimics and inhibitors. *Curr. Opin. Chem. Biol.* **2001**, *5*, 654−659.

(9) Toogood, P. L. Inhibition of protein−protein association by small molecules: Approaches and progress. *J. Med. Chem.* **2002**, *45*, 1543−1558.

(10) Yin, H.; Hamilton, A. D. Strategies for targeting protein−protein interactions with synthetic agents. *Angew. Chem., Int. Ed.* **2005**, *44*, 4130−4163.

(11) Braisted, A. C.; Oslob, J. D.; Delano, W. L.; Hyde, J.; McDowell, R. S.; Waal, N.; Yu, C.; Arkin, M. R.; Raimundo, B. C. Discovery of a potent small molecule IL-2 inhibitor through fragment assembly. *J. Am. Chem. Soc.* **2003**, *125*, 3714−3715.

(12) Yin, H.; Lee, G. I.; Sedey, K. A.; Kutzki, O.; Park, H. S.; Omer, B. P.; Ernst, J. T.; Wang, H. G.; Sebti, S. M.; Hamilton, A. D. Terphenyl-based bak BH3 alpha-helical proteomimetics as low-molecular-weight antagonists of Bcl-X-L. *J. Am. Chem. Soc.* **2005**, *127*, 10191−10196.

(13) Lesuisse, D.; Lange, G.; Deprez, P.; Benard, D.; Schoot, B.; Delettre, G.; Marquette, J. P.; Broto, P.; Jean-Baptiste, V.; Bichet, P.; Sarubbi, E.; Mandine, E. SAR and X-ray. A new approach combining fragment-based screening and rational drug design: Application to the discovery of nanomolar inhibitors of Src SH2. *J. Med. Chem.* **2002**, *45*, 2379−2387.

(14) Zeng, L.; Li, J. M.; Muller, M.; Yan, S.; Mujtaba, S.; Pan, C. F.; Wang, Z. Y.; Zhou, M. M. Selective small molecules blocking HIV-1 Tat and coactivator PCAF association. *J. Am. Chem. Soc.* **2005**, *127*, 2376−2377.

(15) Becattini, B.; Sareth, S.; Zhai, D. Y.; Crowell, K. J.; Leone, M.; Reed, J. C.; Pellecchia, M. Targeting apoptosis via chemical design: Inhibition of bid-induced cell death by small organic molecules. *Chem. Biol.* **2004**, *11*, 1107−1117.

(16) Kussie, P. H.; Gorina, S.; Marechal, V.; Elenbaas, B.; Moreau, J.; Levine, A. J.; Pavletich, N. P. Structure of the MDM2 oncoprotein bound to the p53 tumor suppressor transactivation domain. *Science* **1996**, *274*, 948−953.

(17) Bottger, V.; Bottger, A.; Howard, S. F.; Picksley, S. M.; Chene, P.; Garcia-Echeverria, C.; Hochkeppel, H. K.; Lane, D. P. Identification of novel mdm2 binding peptides by phage display. *Oncogene* **1996**, *13*, 2141−2147.

(18) Garcia-Echeverria, C.; Chene, P.; Blommers, M. J. J.; Furet, P. Discovery of potent antagonists of the interaction between human double minute 2 and tumor suppressor p53. *J. Med. Chem.* **2000**, *43*, 3205−3208.

(19) Stoll, R.; Renner, C.; Hansen, S.; Palme, S.; Klein, C.; Belling, A.; Zeslawski, W.; Kamionka, M.; Rehm, T.; Muhlhahn, P.; Schumacher, R.; Hesse, F.; Kaluza, B.; Voelter, W.; Enhh, R. A.; Holak, T. A. Chalcone derivatives antagonise interactions between the human oncoprotein MDM2 and p53. *Biochemistry* **2001**, *40*, 336−344.

(20) Zhao, J. H.; Wang, M. J.; Chen, J.; Luo, A. P.; Wang, X. Q.; Wu, M.; Yin, D. L.; Liu, Z. H. The initial evaluation of nonpeptidic small-molecule HDM2 inhibitors based on p53−HDM2 complex structure. *Cancer Lett.* **2002**, *183*, 69−77.

(21) Majeux, N.; Scarsi, M.; Caflisch, A. Efficient electrostatic solvation model for protein-fragment docking. *Proteins* **2001**, *42*, 256−268.

(22) Duncan, S. J.; Gruschow, S.; Williams, D. H.; McNicolas, C.; Purewal, R.; Hajek, M.; Gerlitz, M.; Martin, S.; Wrigley, S. K.; Moore, M. Isolation and structure elucidation of chlorofusin, a novel p53-MDM2 antagonist from a *Fusarium* sp. *J. Am. Chem. Soc.* **2001**, *123*, 554−560.

(23) Chene, P.; Fuchs, J.; Bohn, J.; Garcia-Echeverria, C.; Furet, P.; Fabbro, D. A small synthetic peptide, which inhibits the p53−hdm2 interaction, stimulates the p53 pathway in tumour cell lines. *J. Mol. Biol.* **2000**, *299*, 245−253.

(24) Vassilev, L. T.; Vu, B. T.; Graves, B.; Carvajal, D.; Podlaski, F.; Filipovic, Z.; Kong, N.; Kammlott, U.; Lukacs, C.; Klein, C.; Fotouhi, N.; Liu, E. A. In vivo activation of the p53 pathway by small-molecule antagonists of MDM2. *Science* **2004**, *303*, 844−848.

(25) Grasberger, B. L.; Lu, T. B.; Schubert, C.; Parks, D. J.; Carver, T. E.; Koblish, H. K.; Cummings, M. D.; LaFrance, L. V.; Milkiewicz, K. L.; Calvo, R. R.; Maguire, D.; Lattanze, J.; Franks, C. F.; Zhao, S. Y.; Ramachandren, K.; Bylebyl, G. R.; Zhang, M.; Manthey, C. L.; Petrella, E. C.; Pantoliano, M. W.; Deckman, I. C.; Spurlino, J. C.; Maroney, A. C.; Tomczuk, B. E.; Molloy, C. J.; Bone, R. F. Discovery and cocrystal structure of benzodiazepinedione HDM2 antagonists that activate p53 in cells. *J. Med. Chem.* **2005**, *48*, 909−912.

(26) Parks, D. J.; LaFrance, L. V.; Calvo, R. R.; Milkiewicz, K. L.; Gupta, V.; Lattanze, J.; Ramachandren, K.; Carver, T. E.; Petrella, E. C.; Cummings, M. D.; Maguire, D.; Grasberger, B. L.; Lu, T. B. 1,4-Benzodiazepine-2,5-diones as small molecule antagonists of the HDM2−p53 interaction: discovery and SAR. *Bioorg. Med. Chem. Lett.* **2005**, *15*, 765−770.

(27) Geiger, T.; Husken, D.; Weiler, J.; Natt, F.; Woods-Cook, K. A.; Hall, J.; Fabbro, D. Consequences of the inhibition of Hdm2 expression in human osteosarcoma cells using antisense oligonucleotides. *Anti-Cancer Drug Des.* **2000**, *15*, 423−430.

(28) Meye, A.; Wurl, P.; Bache, M.; Bartel, F.; Grunbaum, U.; Mansaard, J.; Schmidt, H.; Taubert, H. Colony formation of soft tissue sarcoma cells is inhibited by lipid-mediated antisense oligodeoxynucleotides targeting the human mdm2 oncogene. *Cancer Lett.* **2000**, *149*, 181−188.

(29) Chen, L.; Agrawal, S.; Zhou, W.; Zhang, R.; Chen, J. Synergistic activation of p53 by inhibition of *MDM2* expression and DNA damage. *Proc. Natl. Acad. Sci. U.S.A.* **1998**, *95*, 195−200.

(30) Wasylyk, C.; Salvi, R.; Argentini, M.; Dureuil, C.; Delumeau, I.; Abecassis, J.; Debussche, L.; Wasylyk, B. p53 mediated death of cells overexpressing MDM2 by an inhibitor of MDM2 interaction with p53. *Oncogene* **1999**, *18*, 1921−1934.

(31) Chene, P.; Fuchs, J.; Carena, I.; Furet, P.; Echeverria, C. G. Study of the cytotoxic effect of a peptidic inhibitor of the p53−hdm2 interaction in tumor cells. *FEBS Lett.* **2002**, *529*, 293−297.

(32) Hardcastle, I. R.; Ahmed, S. U.; Atkins, H.; Farnie, G.; Golding, B. T.; Griffin, R. J.; Guyenne, S.; Hutton, C.; Källblad, P.; Kemp, S. J.; Kitching, M. S.; Newell, D. R.; Norbedo, S.; Northen, J. S.; Reid, R. J.; Saravanan, K.; Willems, H. M. G.; Lunec, J. Isoindolinone based inhibitors of the MDM2−p53 protein−protein interaction. *Bioorg. Med. Chem. Lett.* **2005**, *15*, 1515−1520.

(33) Paull, K. D.; Shoemaker, R. H.; Hodes, L.; Monks, A.; Scudiero, D. A.; Rubinstein, L.; Plowman, J.; Boyd, M. R. Display and analysis of patterns of differential activity of drugs against human tumor cell lines: development of mean graph and COMPARE algorithm. *J. Natl. Cancer Inst.* **1989**, *81*, 1088−1092.

(34) Mancera, R. L.; Källblad, P.; Todorov, N. P. Ligand-protein docking using a quantum stochastic tunneling optimization method. *J. Comput. Chem.* **2004**, *25*, 858−864.

(35) Källblad, P.; Mancera, R. L.; Todorov, N. P. Assessment of multiple binding modes in ligand-protein docking. *J. Med. Chem.* **2004**, *47*, 3334−3337.

(36) Jones, G.; Willett, P.; Glen, R. C.; Leach, A. R.; Taylor, R. Development and validation of a genetic algorithm for flexible docking. *J. Mol. Biol.* **1997**, *267*, 727−748.

(37) Stahl, M.; Todorov, N. P.; James, T.; Mauser, H.; Boehm, H. J.; Dean, P. M. A validation study on the practical use of automated de novo design. *J. Comput.-Aided Mol. Des.* **2002**, *16*, 459−478.

(38) Kitching, M. S.; Clegg, W.; Elsegood, M. R. J.; Griffin, R. J.; Golding, B. T. Synthesis of 3-alkoxy and 3-alkylamino-2-alkyl-3-arylisoindolinones. *Synlett* **1999**, 997−999.

(39) Sayle, K. L.; Bentley, J.; Boyle, F. T.; Calvert, A. H.; Cheng, Y. Z.; Curtin, N. J.; Endicott, J. A.; Golding, B. T.; Hardcastle, I. R.; Jewsbury, P.; Mesguiche, V.; Newell, D. R.; Noble, M. E. M.; Parsons, R. J.; Pratt, D. J.; Wang, L. Z.; Griffin, R. J. Structure-based design of 2-arylamino-4-cyclohexylmethyl-5-nitroso-6-aminopyrimidine inhibitors of cyclin-dependent kinases 1 and 2. *Bioorg. Med. Chem. Lett.* **2003**, *13*, 3079−3082.

(40) Douglas, N. L.; Ley, S. V.; Lucking, U.; Warriner, S. L. Tuning glycoside reactivity: New tool for efficient oligosaccharide synthesis. *J. Chem. Soc., Perkin Trans. 1* **1998**, 51−65.

(41) Orndorff, W. R.; Murray R. R. A new class of phthaleins—mixed phthaleins—formed by heating *p*-hydroxy-*o*-benzoic acids with phenols. *J. Am. Chem. Soc.* **1917**, *39*, 679−697.

(42) Maple, J. R.; Dinur, U.; Hagler, A. T. Derivation of force-fields for molecular mechanics and dynamics from ab initio energy surfaces. *Proc. Natl. Acad. Sci. U.S.A.* **1988**, *85*, 5350−5354.

(43) Todorov, N. P.; Dean, P. M. Evaluation of a method for controlling molecular scaffold diversity in de novo ligand design. *J. Comput.-Aided Mol. Des.* **1997**, *11*, 175−192.

(44) Kallblad, P.; Todorov, N. P.; Willems, H. M. G.; Alberts, I. L. Receptor flexibility in the in silico screening of reagents in the S1′ pocket of human collagenase. *J. Med. Chem.* **2004**, *47*, 2761−2767.

(45) Firth-Clark, S.; Willems, H. M. G.; Williams, A.; Harris, W. Generation and selection of novel estrogen receptor ligands using the de novo structure-based design tool, SkelGen. *J. Chem. Inf. Comput. Sci.* **2006**, *46*, 642−647.

(46) Bondi, A. Van der Waals volumes and radii. *J. Phys. Chem.* **1968**, *68*, 441−451.

(47) Bohm, H. J. The development of a simple empirical scoring function to estimate the binding constant for a protein ligand complex of known 3-dimensional structure. *J. Comput.-Aided Mol. Des.* **1994**, *8*, 243−256.

(48) Todorov, N. P.; Dean, P. M. A branch-and-bound method for optimal atom-type assignment in de novo ligand design. *J. Comput.-Aided Mol. Des.* **1998**, *12*, 335−349.

(49) Liang, H.; Lunec, J. Characterisation of a novel p53 down-regulated promoter intron 3 of the human MDM2 oncogene. *Gene* **2005**, *361*, 112−118.